Proceedings of ASME Turbo Expo 2016: Turbomachinery Technical Conference and Exposition
GT2016
June 13 – 17, 2016, Seoul, South Korea

GT2016-57784

PARAMETRIC GEOMETRY AND CFD PROCESS FOR TURBOFAN NACELLES

Alexander Heidebrecht*
Propulsion Engineering Centre
School of Aerospace, Transport, and Manufacturing
Cranfield University
Bedfordshire, MK43 0AL, UK
Email: a.heidebrecht@cranfield.ac.uk

Tomasz Stańkowski
David MacManus
Propulsion Engineering Centre
School of Aerospace, Transport, and Manufacturing
Cranfield University
Bedfordshire, MK43 0AL, UK

ABSTRACT

A parametric geometry definition for a generic turbofan nacelle was developed for use in preliminary design, based on Class-Shape Transformation curves. This takes as input a set of six intuitive variables which describe the main dimensions of a nacelle. This set is the same set of inputs as required by a preliminary nacelle design method to which the aerodynamic properties of resulting shapes were compared. An automated computational fluid simulation process was developed and implemented which generates meshes and quickly conducts an analysis of the resulting nacelle shapes using a commercial code. Several geometries were generated and analysed using this process to show whether the aerodynamic properties of the generated shapes are in line with the expected performance of a fan cowl of equal dimensions. It was found that the aerodynamic performance of the parametric fan cowls significantly exceeds predictions from an established preliminary fan cowl design method and is very close in performance to existing designs. The drag of an equivalent parametric fan cowl can therefore be used as a predictor of nacelle performance with greater accuracy than established preliminary design methods. It is therefore suited as a tool to develop improved preliminary design methods, and for studies of the design space for preliminary nacelle design.

*Address all correspondence to this author.

NOMENCLATURE

Abbreviations

CFD	Computational Fluid Dynamics
CRM	Common Research Model
CST	Class-Shape Transformation
GCI	Grid Convergence Index
PD	Preliminary Design
TFN	Through-Flow Nacelle

Symbols

A	area
BP	Bernstein polynomial
bp	Bernstein polynomial weighting coefficient
C	class function
c	chord length
c_D	drag coefficient
$c_{D,ref}$	drag at reference conditions (M=0.5, MFCR=1.0)
f_{if}	non-dimensional initial forebody radius
f_{max}	non-dimensional position of maximum nacelle radius
$g_1 ... g_6$	non-dimensional fan cowl design variables
i	index of summation
K	binomial coefficient
l_{nac}	nacelle length
M	Mach number
M_{DR}	drag rise Mach number
$MFCR$	mass-flow capture ratio
N	number of points in a CFD grid

n	degree of Bernstein polynomial
P	pressure
r	radial coordinate
r_{FF}	radius of the far-field domain
r_{if}	initial forebody radius: radius of curvature at nacelle highlight
r_{max}	maximum nacelle radius
S	shape function
T	temperature
x	axial coordinate, ordinate
y	abscissa
β_{nac}	boat-tail angle
ψ	non-dimensional abscissa
ξ	non-dimensional ordinate

Indices

∞	at upstream infinity
hi	nacelle highlight
T	total quantity
te	nacelle trailing edge

INTRODUCTION

Due to constantly increasing bypass ratios, engine integration in general and nacelle design in particular is becoming an increasingly important tool to minimize the aerodynamic penalty of cowls around ever larger fans. In this context, nacelle drag needs to be regarded early on in the engine design process in order to weigh the benefits of increasing bypass ratio against the increase in nacelle drag. However, preliminary design (PD) methods for nacelles are based on limited experimental data obtained from either NACA1-type nacelle geometries or variations of these [1] [2], which may not be representative of modern nacelles.

Class-Shape-Transformation (CST) curves [3] can be used to construct aerodynamically beneficial shapes and have so far mostly been applied to airfoil geometries [4]. It has been found that they are especially suited for preliminary airfoil design purposes since they can model smooth shapes with fewer degrees of freedom than alternative curve types [5]. CST curves have also been suggested for representation of podded engine nacelles [6]. This has been applied for full optimisation scenarios of inlet ducts [7], though not for the purpose of preliminary design of fan cowls.

The aim of this work is to develop a parametric geometry definition for a generic turbofan nacelle to study preliminary design problems of fan cowl geometries. The geometry of both fan cowl and intake is based on CST curves whose coefficients are computed to match a set of constraints on the curve which reflect the values of six intuitive design variables, using the method described by Christie et al. [8]. An efficient CFD model to rapidly assess drag of axisymmetric nacelles across a range of operating conditions was developed and validated. An automated CFD process was then implemented to generate geometries and meshes, and to conduct drag analyses for different geometries. Using these tools, an analysis of the drag characteristics of the parametric geometry was conducted to test its utility for preliminary design studies. Since preliminary design attempts to predict the performance of a finished design from a reduced set of design variables, the aerodynamic performance of the generated shapes needs to be close to that of fully optimised designs, and the offset in performance between full designs and the simpler parametric shapes should be consistent within the design space. This means that while absolute nacelle drag of the simpler shapes may not be equal to that of a full design, the effects of design changes on drag should be represented well in the simplified model.

The preliminary design method described in ESDU/ 81024 [1] was used as a baseline for a preliminary design code. It is mainly based on the performance of NACA1-type fan cowls which have 5 design variables. For predictions below below M=0.6, it also includes data from nacelles with different forebody geometries [9], based on the same 6 design variables used to construct the parametric geometry introduced in this paper. This code was used as a low-order comparison which an improved PD method should be able to outperform, thus the parametric fan cowls are expected to have better properties than predicted by the ESDU code.

As a higher-order baseline, an existing design for a throughflow nacelle was used. This tests the ability of the parametric geometry to generate shapes which approximate the drag characteristics of a realistic existing design, based on the same 6 variables used by the preliminary design code.

METHODOLOGY

CST curves

Class Shape Transformation (CST) curves [3] are the product of a class function, $C(\psi)$, and a shape function, $S(\psi)$, added to a term which determines the vertical offset between the endpoints [3]:

$$\xi(\psi) = S(\psi)C(\psi) + \psi\Delta\xi_{te} \quad ; \quad \xi = \frac{y}{c} \ , \ \psi = \frac{x}{c} \qquad (1)$$

The class function defines a basic profile, to which the shape function is then applied as a modifier. The class function used in this study is suggested for airfoil shapes [3]:

$$C(\psi) = \psi[1-\psi]^{0.5} \ for \ 0 \leq \psi \leq 1 \qquad (2)$$

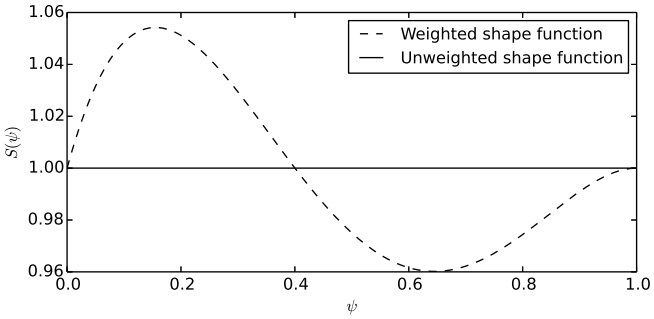

FIGURE 1: Example of a shape function based on a Bernstein polynomial with weighting coefficients

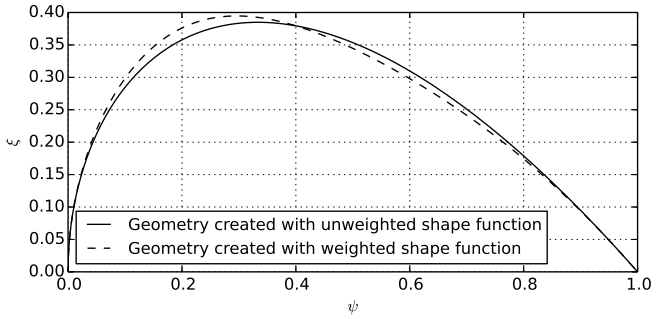

FIGURE 2: Geometry created with a unit shape function (thus equal to class function) and with a shape function perturbed by Bernstein polynomial weighting coefficients (Figure 1)

As the shape function, Bernstein polynomials (Eqn. 3) are commonly employed [3, 6, 10].

$$BP(\psi) = \sum_{i=0}^{n} \left[K_{i,n} \cdot \left(\psi^i \cdot (1-\psi)^{n-1} \right) \right] \; ; \; K_{i,n} = \frac{n!}{i!(n-1)!} \quad (3)$$

The Bernstein polynomial forms a partition of unity, independent of its order n, i.e., the $n+1$ Bernstein polynomials sum to one, while the contributions of the individual terms change with ψ. The shape function can be defined by applying coefficients to the individual terms in the Bernstein polynomial function (Eqn. 4). Becausue the terms in the Bernstein polynomial are infinitely derivable, this always creates an infinitely derivable, smooth curve (example: see Figure 1).

$$S(\psi) = \sum_{i=0}^{n} \left[bp_i \cdot K_{i,n} \cdot \left(\psi^i \cdot (1-\psi)^{n-1} \right) \right] \quad (4)$$

Multiplying the shape function shown in Figure 1 with the basic airfoil class function (Eqn. 2) results in the combined shape shown in Figure 2.

Parametric Geometry

The parametric fan cowl geometry definition aims to represent the external aero-lines of a nacelle with as few variables as possible while allowing for realistic shapes. Because the parametric fan cowls have relatively few design variables, an offset in aerodynamic performance between the resulting shapes and fully optimised designs is unavoidable. While such an offset should be small, it is acceptable in preliminary design as long as it consistently reflects the effects of design changes on performance. The main geometric dimensions which impact aerodynamic fan cowl performance were identified and are shown in Figure 3.

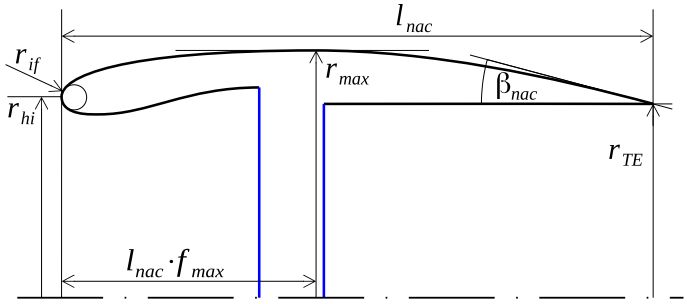

FIGURE 3: The parameters used to specify the nacelle geometry

Of these measures, r_{hi}, r_{te} and l_{nac} are used to define the endpoints of the fan cowl curve. The other parameters are used to derive constraints on a 5th order CST curve which forms the fan cowl geometry: r_{if} constrains the curvature at the leading edge; r_{max} constrains the function value at position $l_{nac} \cdot f_{max}$ and the tangent at this point; The boat-tail angle β_{nac} determines the tangent at the trailing edge. The applied constraints are shown in Figure 4. In addition to the constraints which enforce the design variables, curvature at the nacelle trailing edge was constrained to zero, independent of the design variables. This additional constraint was found to create more consistent geometries than unconstrained curvature. Zero curvature at the trailing edge also allows curvature-continuous blending with conical extensions. In aerodynamic terms, the effect of reducing curvature is to increase the pressure coefficient at the trailing edge, which decreases drag.

To allow investigation of the fan cowl shapes, intake aerolines had to be created as well. Since intake performance was not part of the investigation, the parameterisation and the design was chosen with the aim of creating a neutral intake which has as little influence on flow over the fan cowl as possible, and is able to operate at as large a range of mass-flows and Mach numbers as

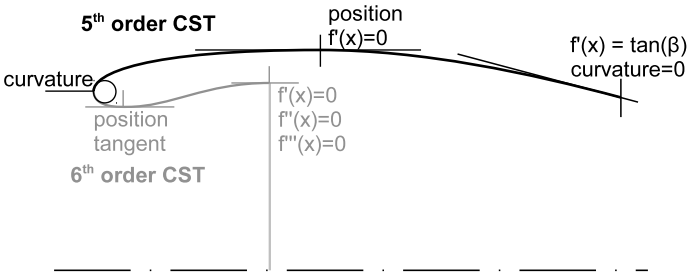

FIGURE 4: Constraints used to impose the parameters shown in Figure 3

possible. The design also needs to be consistently independent of fan cowl design. The parameterisation uses a similar approach as for the fan cowl (see Figure 4). Curvature across the highlight was equal to that of the fan cowl to avoid a jump in curvature which might affect fan cowl performance. The contraction ratio from highlight to throat was set to 1.25, to allow investigation of large mass-flow capture ratios without choking the intake. The length of the intake was chosen to be about 1.4 times the highlight radius, which allows for a long diffuser, and the throat was positioned at approximately 20% of intake length. The fan radius was chosen to be 98% of the highlight radius. The intake curve parametrisation constrains curvature at the highlight, location and tangent at the throat, and tangent at the downstream end. In addition, both second and third derivative of the diffuser at the fan face were constrained to zero. While this may have a slight negative impact on diffuser performance, it was found that it helps to avoid unwanted additional inflections of the curve and made resulting diffuser geometries less dependent on r_{if}. Within this study the geometric proportions given above were kept constant. This way the intake geometry is always scaled to the highlight diameter with matching curvature at the highlight, to achieve the goal of generating intake lines which behave consistently and do not interfere with the flow on the fan cowl.

A software tool was written in Python which implements the parametrisation. It uses the method of analytical CST curve-fitting shown by Christie et al. [8] to determine the Bernstein coefficients required to fit curves to the constraints using an analytical approach, and outputs fan cowl and intake geometries for mesh generation.

To generalise the parameterisation described above, a set of non-dimensional design variables was defined, based on the dimensional values shown in Figure 3. The non-dimensional variables are shown in Table 1. Maximum radius and nacelle length are simply referenced to highlight radius; f_{max} is already non-dimensional. The non-dimensional variable for the initial forebody radius, f_{if}, is a generalisation of the definition of NACA1-type forebodies [11] ($f_{if} = 0.546$ for NACA1-type fore-bodies). The non-dimensionalized trailing edge radius is defined as the slope of a straight line formed by the highlight and trailing edge points. The boat-tail angle is given in degrees. The absolute dimensions of a nacelle are defined by the six non-dimensional design variables in Table 1 in combination with the dimensional highlight radius r_{hi}.

variable	definition	Description
g_1	$\frac{r_{max}}{r_{hi}}$	maximum radius
g_2	$\frac{l_{nac}}{r_{hi}}$	nacelle length
g_3	f_{max}	location of maximum radius
g_4	$f_{if} = \frac{r_{if} \cdot f_{max} l_{nac}}{(r_{max} - r_{hi})^2}$	initial forebody radius
g_5	$\frac{r_{te} - r_{hi}}{l_{nac}}$	trailing edge radius
g_6	$\beta_{nac}/^\circ$	boat-tail angle

TABLE 1: Non-dimensional design variables for the parametric fan cowl geometry

Simulation Methodology

The following sections explain how the simulations of fan cowl performance were conducted, which boundary conditions were used and which definition for nacelle drag was applied. To assure reliable results, both a domain sensitivity study and a mesh convergence study were conducted.

CFD Solver ANSYS Fluent v15 [12] was used as the CFD solver. Computations were carried out using the Reynolds-Averaged Navier-Stokes, implicit, density-based approach coupled with the SST k-ω turbulence model. Air was modelled as an ideal compressible gas according to kinetic theory. Variable viscosity was calculated using Sutherlands law. The solution method was a cell-centered implicit time-stepping scheme using the Roe-FDS scheme for flux calculation, and Green-Gauss node-based gradient evaluation. Second order, upwind discretisations were utilised for the convection terms. Solutions were deemed to be converged when all scaled residuals reached a value below 1×10^{-5} and coefficients for forces on all walls were either constant or not oscillating by more than 10^{-5} over 100 iterations.

2D axisymmetric CFD model To allow sufficiently quick turnaround of simulation results, all nacelle geometries were regarded as 2D axisymmetric, thus no incidence effects were regarded. This is sufficient to extract the main drag characteristics of a design and is a common simplification in preliminary design contexts [1, 2]. The geometry incorporates nacelle

and intake lines created using the parametric CST shapes described above. At the position of the fan, a pressure-exit boundary condition was employed. Predefined mass-flow capture ratios were simulated by setting target mass-flow according to the MFCR and ambient conditions. This causes the solver to iterate on the exit pressure to achieve the desired mass-flow. For the rear of the nacelle, a datum nozzle geometry was used, which consists of a total-pressure inflow boundary condition and cylindrical, inviscid walls. The total pressure and temperature specified at the boundary is the same as on the far field, thus the outflow velocity of the expanded nozzle stream is equal to the ambient velocity. The configuration is shown in Figure 5.

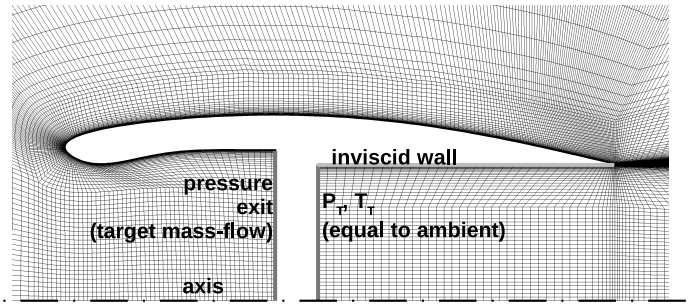

FIGURE 5: View of one of the two-dimensional axisymmetric meshes used in this study, representing fan cowl and intake, indicating boundary conditions used in the simulations

Domain Sensitivity Study The flow domain was defined using a semi-circular far-field boundary. Four different radii of the far field (r_{FF}) were used for the domain sensitivity study: 60, 70, 80 and 90 times the maximum nacelle radius (r_{max}). Figure 6 shows extracted nacelle drag as a function of the domain size. Moving from $r_{FF}/r_{max} = 70$ to $r_{FF}/r_{max} = 80$ only incurs a relative change below 0.004%, therefore $r_{FF}/r_{max} = 80$ was accepted as a sufficient domain size.

Meshing For meshing of 2D axisymmetric cases, ANSYS ICEM CFD [13] was used to create fully structured meshes for nacelle geometries. The boundary layer blocks on fan cowl and intake use 50 cells and the first wall distance results in a y_1^+ below 1. In order to capture and resolve compressible shocks on the fan cowl, the maximum element size on the surface was limited to 1/110th of the nacelle length, resulting in 190 cells along the outside of a nacelle. The intake duct was resolved with 112 cells in radial direction. Figure 5 shows one of the 2D meshes used in this study, which has approximately 39000 cells.

A grid convergence study was conducted using during which the mesh density was both doubled and halved in all directions,

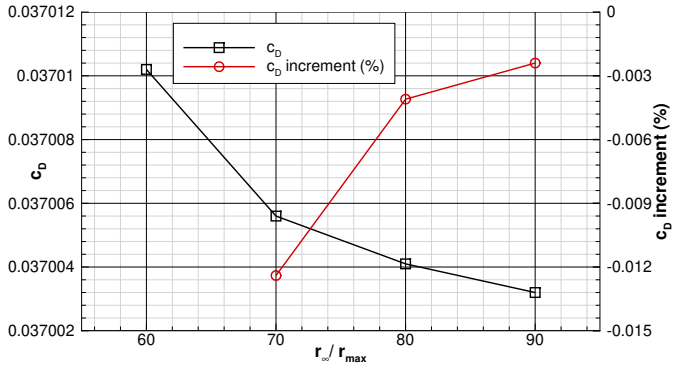

FIGURE 6: Nacelle drag variation over ratio of domain radius to maximum nacelle radius. "Drag increment" is the relative change of drag from the next smaller domain size.

resulting in a coarse mesh of 11000 cells and a fine mesh of 155000 cells. Figure 7 shows the development of nacelle drag over mesh density. It can be seen that all three meshes are in the asymptotic range since the drag does scale linearly with the inverse of the number of points. In this case, Roache [14] recommends calculating the Grid Convergence Index (GCI) using Equations 5 and 6, depending on whether the fine or the coarse grid density is being used:

$$GCI_{fine} = 1.25 \frac{c_{D,fine} - c_{D,coarse}}{c_{D,fine}\left(r^p - 1\right)} \tag{5}$$

$$GCI_{coarse} = 1.25 r^p \frac{c_{D,fine} - c_{D,coarse}}{c_{D,coarse}\left(r^p - 1\right)} \tag{6}$$

In Equations 5 and 6, r is the ratio of cell sizes (2 in this study), and p is the order of the numeric method (also 2 in this case). For the medium grid, the result is 1.1% when using the coarse and medium grid in Equation 5, and 0.9% when applying Equation 6 to the medium and fine grid. The estimated grid convergence error was deemed acceptable, and the medium mesh was used in all further CFD simulations.

Calculations and Drag Extraction Each of the parametric fan cowl geometries analysed in this report was simulated at a range of operating conditions, varying the Mach number between 0.2 and 0.95. The mass-flow into the nacelle is given as mass-flow capture ratio, defined in Equation 7 as the ratio between the cross-section area of the intake streamtube at upstream

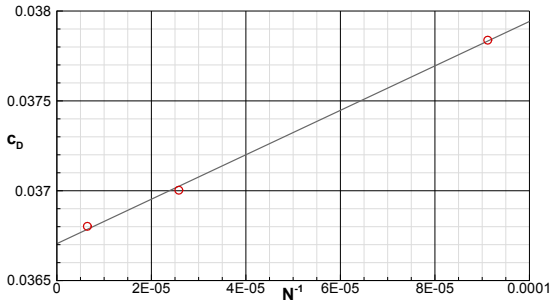

FIGURE 7: Influence of number of cells in the grid (N) on nacelle drag. Inverse scaling for second-order accurate code in two dimensions

infinity and at the highlight area.

$$MFCR = \frac{A_\infty}{A_{hi}} \tag{7}$$

The maximum achievable mass-flow capture ratio is Mach number-dependent because the mass-flow which can pass through the intake throat without choking the intake depends on upstream Mach number. Therefore the range of mass-flow capture ratios was taken from 0.3 to 95% of the theoretical maximum at any given Mach number. A Python script was written which produces journal files for Fluent to conduct simulations and output results at 224 separate operating conditions within the specified range. The results of these simulations were combined to form a drag map which contains the modified standard nacelle drag coefficient as a function of Mach number and MFCR. Due to re-use of previous solutions, the solution time for one drag map was less than 12 hours on a single compute cluster node using two 6-core Intel Xeon E5620 processors.

For fan cowl drag extraction from the simulations, the method shown by Christie [15] was used. This extracts the modified standard nacelle drag [16], which consists of the forces on intake streamtube and fan cowl but does not regard post-exit forces. Nacelle drag figures in this paper are given as drag coefficients relative to the nacelle highlight area, using far-field dynamic pressure.

During test calculations it was found that the choice of nozzle geometry and boundary condition has a non-negligible influence on the drag extracted from the solution. This makes it impossible to directly compare nacelle drag from different sources which use different nozzle configurations. The datum nozzle was chosen to achieve a neutral flow with minimal post-exit forces. This means minimizing jet entrainment effects by removing the jet and reducing pressure forces on the nacelle afterbody by creating a nozzle flow as parallel to the axis as possible. The former is achieved by specifying ambient total values at the influx boundary, the latter cannot be completely achieved since the fan cowl geometry is not axis-parallel. Figure 8 shows the shape of the nozzle streamtube and the Mach number distribution. It can be seen that the streamtube contracts slightly downstream of the nacelle, and that pressure in the nozzle plane is increased compared to far-field conditions. This pressure increase cannot be avoided and depends both on the boat-tail angle and on the displacement of the exit streamtube. Compared to the datum nozzle setup, an engine with separate exhausts will produce a jet of smaller displacement, and thus lower pressure in the nozzle plane. However, wind tunnel measurements of nacelle drag often employ a straight cylindrical sting [17] which has a larger displacement, thus creates a stronger pressure increase in the nozzle plane.

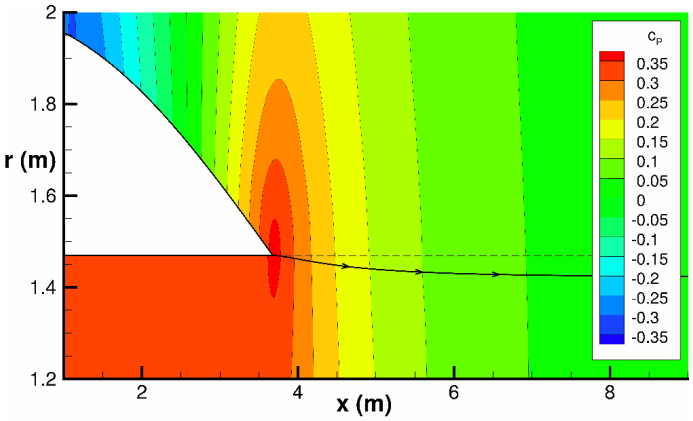

FIGURE 8: Flow around the rear of a datum-nozzle nacelle at $M_\infty = 0.86$ (vertical and horizontal coordinates use different scales). The streamtrace shows the boundary between nozzle flow and exterior flow field.

These effects cause an offset in nacelle drag data produced in wind tunnels, such as the data used to derive the correlations in the preliminary design code ESDU 81024 [1], compared to drag figures from simulations using either datum nozzles or separate exhausts. For this reason, drag comparisons between the CFD model and the preliminary design code were not conducted on raw drag figures but the difference between drag and reference drag which is defined in this paper as the drag of a given nacelle at M=0.5, MFCR=1.0. Where several datasets from CFD and the ESDU method are compared, all results from one method use the same reference drag appropriate for the method. This is done to preserve the ability to compare changes of reference drag within the two groups of datasets.

RESULTS

Several nacelle shapes were generated and their aerodynamic properties analysed to investigate the properties of the parametric geometry definition. The effects of most of the design variables shown in Figure 3 have been studied and published for NACA1-type cowls [1, 2], and are therefore input variables for the preliminary design code. The initial forebody radius (r_{if}) for these fan cowls is fixed or is only investigated on a limited basis. However, r_{if} is an input variable for the proposed parametric geometry. For this reason, a set of geometries with varying r_{if} was regarded and compared geometrically to NACA1 nacelles and to the prediction of the preliminary design code [1]. The results are used to discuss the utility of r_{if} in preliminary design, and the utility of using the proposed parametric nacelle model in the context of preliminary design.

To test the extent to which the parametric fan cowl shapes represent the geometrical and aerodynamical characteristics of final designs of equal proportions, the known geometry of an existing fan cowl was reconstructed from the six measures shown in Figure 3 using the parametric geometry. The resulting drag characteristics are then compared to those of the original shape, and to results from the ESDU 81024 method [1], using the same variables as input. The indicators used in this comparison were spillage curves at subsonic Mach number (0.5), at transonic Mach number (0.82), and the wave drag rise curve at cruise MFCR (0.75).

Variation of initial forebody radius

The ESDU preliminary design code can make predictions in the transonic regime only for nacelles of the NACA1-type. These have a fixed $f_{if} = 0.546$. To investigate how initial forebody radius affects the transonic characteristics of the parametric fan cowls, a comparison was conducted with three different f_{if} but otherwise constant design variables. The variables chosen are shown in Table 2.

var.	definition	A	B	C
g_1	$\frac{r_{max}}{r_{hi}}$	1.246	”	”
g_2	$\frac{l_{nac}}{r_{hi}}$	3.92	”	”
g_3	f_{max}	0.40	”	”
g_4	$f_{if} = \frac{r_{if} \cdot f_{max} l_{nac}}{(r_{max} - r_{hi})^2}$	0.637	0.796	1.115
g_5	$\frac{r_{te} - r_{hi}}{l_{nac}}$	-0.0072	”	”
g_6	$\beta_{nac}/^\circ$	12.0	”	”

TABLE 2: Sets of non-dimensional design variables for comparison between the CFD model and preliminary design code

Geometry The preliminary design method from ESDU [1] is based mostly on measurements on NACA1-type cowls which consist of a forebody derived from NACA1 airfoils [11], a straight cylindrical mid-body and a circular arc transitioning to conical section. Figure 9 shows a comparison of the geometry of the parametric fan cowl generated from dataset B and its curvature distribution with the same data for a NACA1-type fan cowl using the same dataset. The latter geometry is the internal representation of the same geometry configuration in the ESDU code, for predictions in the transonic regime. The parametric design applies a similar but more regular reduction in curvature from the highlight to the mid-body, compared to the NACA1 forebody. Because the CST profile provides continuous curvature over the rear part of the fan cowl rather than using a short circular arc, it does not require as small radii of curvature in the rear region. This is an advantage aerodynamically, because small radii of curvature potentially increase wave drag and the sharp changes in curvature of the NACA1-type nacelle contribute to separation. A possible drawback of the continuous curvature is that the parametric profile offers less internal volume in the rear of the nacelle.

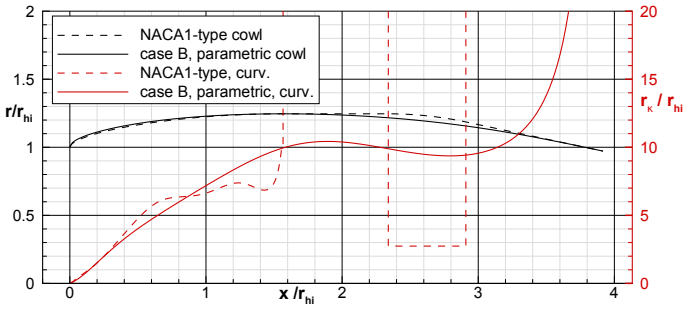

FIGURE 9: Comparison of fan cowl geometry and curvature distribution of the parametric shape and an equivalent NACA1-type fan cowl for dataset B. Radial coordinate and radius of curvature are given as a fraction of highlight radius.

Drag characteristics Parametric shapes were generated using the three sets of design variables in Table 2 and CFD simulations conducted to compute the drag maps for the nacelles. The results were compared to predictions by the ESDU 81024 code for the same sets of input variables. The drag coefficients from the preliminary design code are not directly comparable to those extracted from the CFD simulations with datum nozzle (see section ”Calculations and Drag Extraction”). All CFD results shown in this section use the reference drag coefficient of the parametric fan cowl B as a baseline, while the results from the ESDU

preliminary design code use the reference drag predicted by the ESDU code for the same nacelle.

Figure 10 shows a comparison of spillage drag for the three different nacelles and the corresponding predictions by the ESDU [1] method. While the CFD model does predict modest differences in reference drag (up to 1.5%) between the different geometries, case B having the lowest drag, the ESDU code predicts only minimal differences. The drag slope in all three CFD cases is lower than predicted by the ESDU code, and the sudden rise in spillage drag predicted by the preliminary design code does not occur in the CFD model at all. This prediction is likely due to the fact that the non-curvature-cuntinuous nacelles on which the ESDU method is based show strongly defined separation, while no separations were observed on the curvature-continues parametric nacelles. It should also be noted that the preliminary design code predicts that the onset of spillage drag reduces continuously with increasing initial forebody radius, while CFD only shows this effect between the two first designs and the curves for cases B and C are almost parallel to each other.

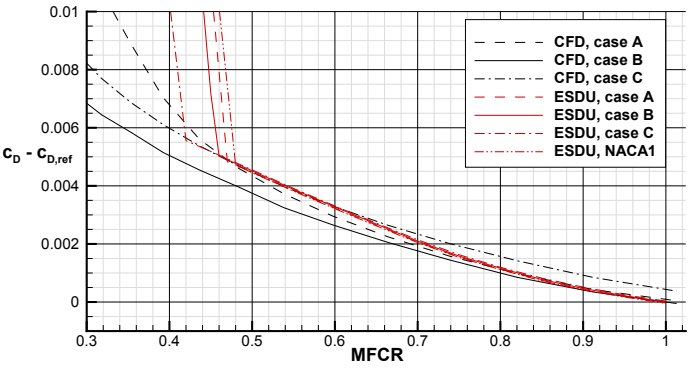

FIGURE 10: CFD results for drag at M=0.5 for the different geometries, and the ESDU 81024 predictions for the same cases as well as the standard NACA1 initial forebody radius.

The CFD results in Figure 10 favour case B, and the results from the preliminary design code confirm that the standard NACA1 forebody radius has disadvantages, even in subsonic conditions, although the PD code finds these differences only at mass-flow capture ratios below 0.5. The results for wave drag rise Mach number are shown in Table 3. At free-stream Mach numbers higher than 0.6, the ESDU method cannot give predictions for non-standard values of f_{if}, therefore the drag rise Mach number prediction from the ESDU code uses the standard NACA1 initial forebody radius. Again the best-performing design in the CFD model is case B. The preliminary design method under-predicts the achievable drag rise Mach number by 0.037. This would not be acceptable in a preliminary design environment and is due to the limitation of the ESDU PD code to NACA1 forebodies, which do not perform well in supercritical flow [17].

case	f_{if}	M_{DR}
ESDU (NACA1)	0.546	0.833
CFD (case A)	0.637	0.857
CFD (case B)	0.796	0.868
CFD (case C)	1.115	0.845

TABLE 3: Drag rise Mach numbers at MFCR=0.75 for the different parametric fan cowls. The ESDU prediction uses $f_{if} = 0.546$ as it cannot assess of M_{DR} for other values.

This confirms that at least for the chosen design variables, the parametric fan cowl geometry can exceed the predictions of established preliminary design methods, based on the same input data. The fact that the initial forebody radius variable is not restricted allows changes to the drag characteristics while keeping the main dimensions of the fan cowl constant. This can be more fully seen by regarding the drag maps for the three different designs, which are shown in Figure 11.

It can be seen that while spillage at low Mach numbers as well as the wave drag rise are slightly modified by the variation in design, the strongest effect is on conditions with low MFCR at transonic Mach numbers. While the two smaller f_{if} settings (case A and B) result in almost equal reference drag, the spillage behaviour suffers at the lower setting, producing an increase of spillage drag at moderate transonic Mach numbers. In case C, the reference drag increases but the interaction between spillage and wave drag at high Mach numbers and low MFCR is changed. Onset of transonic spillage drag at moderate transonic Mach numbers is delayed to about Mach 0.7 (0.6 to 0.65 in the other two cases), but spillage increases steadily with increasing Mach number. At M=0.83, MFCR 0.6, cowl C produces 9% more drag than cowl B. Likewise, drag rise Mach number increases as MFCR is reduced, and both drag rise fronts blend smoothly rather than meeting at an angle as in the first two cases. This observation is in line with the fact that airfoil shapes tend to have more steady characteristics around maximum lift with increasing nose radius, at the cost of higher drag at low incidences.

Overall, it has been shown that given the same input variables, the CFD analysis of the parametric geometry shows considerably better performance than the established PD method. Whereas the PD method only has limited abilities to regard the effect of changes to initial forebody radii, the parametric geometry can use it as an additional degree of freedom which can

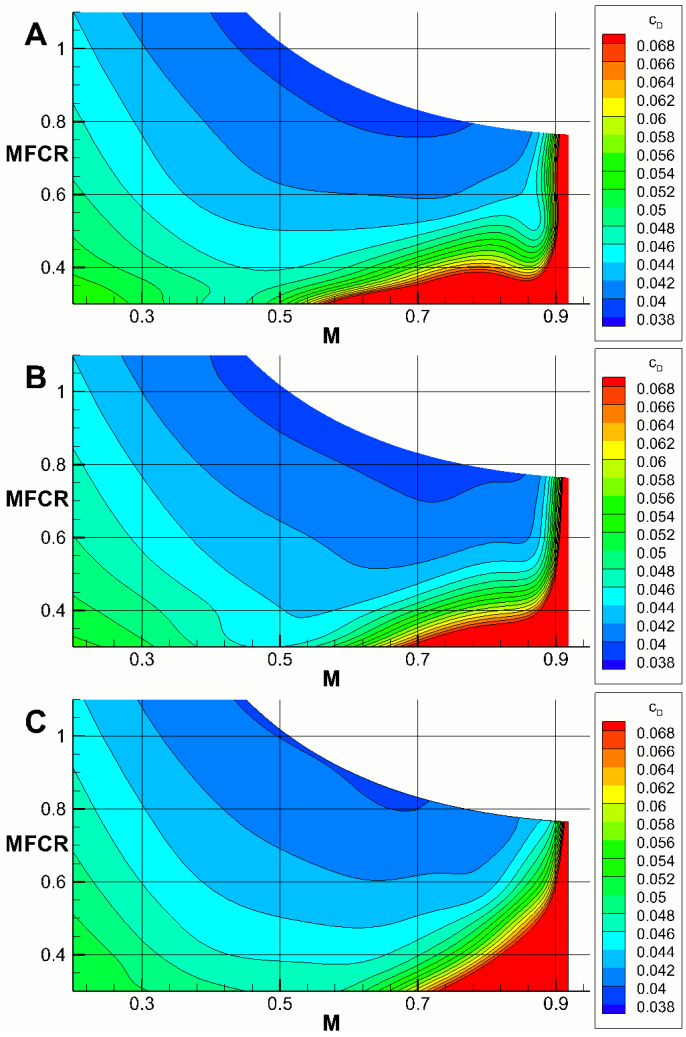

FIGURE 11: CFD drag maps for the parametric nacelles generated from the three sets of design variables.

be used to influence some of the drag characteristics by making trade-offs between drag rise and transonic spillage. It was found that the proposed parametric fan cowl geometry performs best at initial forebody radii well above the standard forebody radius of an equivalent NACA1 forebody. This has been documented [9], but no updated PD method for transonic performance estimates has been published so far. In the investigated case, the best-performing fan cowl uses a 46% higher initial forebody radius than the equivalent NACA1 forebody.

Parametric representation of existing design

The open-source through-flow-nacelle (TFN) of the Common Research Model (CRM) [18, 19] was used as the basis for a comparison of the proposed parametric fan cowl type with an existing design. The fan cowl sideline was extracted from the three-dimensional TFN geometry and used for a CFD analysis. The main dimensions shown in Figure 3 were extracted,used to construct a fan cowl shape using the parametric approach introduced in this paper, and nacelle drag determined via CFD. For comparison, the ESDU preliminary design method [1] was applied to predict nacelle drag using the same input variables.

Geometry The side-line section and all required variables were extracted from the available TFN geometry [19]. For initial forebody radius, curvature analysis did not find a definite value, therefore a value was chosen which lines up the forebody geometries. The resulting design variables are shown in Table 4.

var.	definition	value(s)
g_1	$\frac{r_{max}}{r_{hi}}$	1.207
g_2	$\frac{l_{nac}}{r_{hi}}$	3.60
g_3	f_{max}	0.379
g_4	$f_{if} = \frac{r_{if} \cdot f_{max} l_{nac}}{(r_{max} - r_{hi})^2}$	1.02
g_5	$\frac{r_{te} - r_{hi}}{l_{nac}}$	-0.0318
g_6	$\beta_{nac}/^\circ$	13.27

TABLE 4: Non-dimensional design variables extracted from the CRM through-flow nacelle sideline section

Figure 12 shows a comparison of the original and the reconstructed parametric geometry. It can be seen how the use of just the six main parameters of the nacelle profile results in a shape that closely resembles the original. The largest difference is a deviation of 0.011m on the rear part of the fan cowl, about 0.6% of local radius.

In a preliminary design context, this deviation means that the parametric geometry provides a conservative estimate about the internal volume available for auxiliary units or a thrust reverser. Aerodynamically, it means that the parametric geometry must have reduced curvature on the rear part, compared to the original. This could be brought closer in line by moving the location of maximum radius back, thus lengthening the forebody. However, the goal of the study is not to fit an existing geometry but rather to test whether the parametric fan cowl is able to represent an existing design's aerodynamic properties based on the main dimensions. For this reason, the design variables were not adapted to match the geometry.

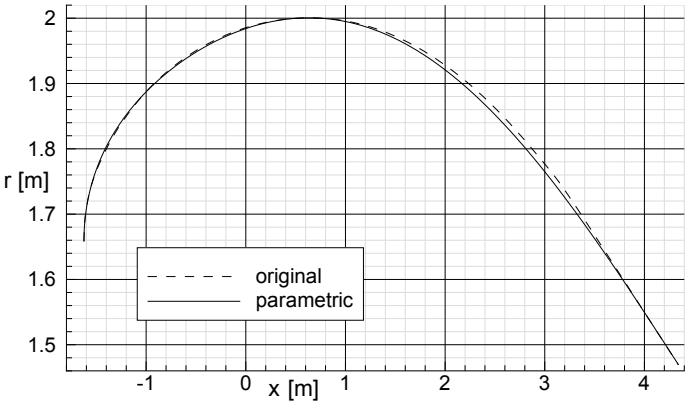

FIGURE 12: Comparison of the original geometry of the CRM TFN sideline and the equivalent fan cowl line constructed using the parametric geometry.

Aerodynamic Performance The ability of the CFD model based on the parametric geometry nacelle to match the aerodynamic properties of the TFN fan cowl was tested by comparing the drag evaluated by CFD for both the original geometry and the parametric model, across the space of operating conditions. To ensure comparable intake conditions, the original CRM fan cowl geometry was joined with the intake and datum nozzle geometry used for the parametric reconstruction. Figure 13 shows the drag maps for both geometries.

Both the overall drag levels and the shape of the drag maps are very similar between the two shapes, however some differences can be observed. The sharp increase of spillage drag at transonic Mach numbers starts at a slightly higher Mach number later (M= 0.6 compared to M=0.54) for the parametric geometry, but increases more with rising Mach number. At Mach 0.8, both fan cowls have almost equal spillage characteristics. Above this, the parametric nacelle has a smaller spillage margin than the original. Considering the influence of initial forebody radius seen in Figure 11, these differences may well be further reduced by adjusting this variable.

Within a preliminary design context, the differences between both cases can be considered to be very small. To quantify this, a drag rise curve and two spillage curves (variations in MFCR) were generated in the ESDU preliminary design code and compared to the CFD data. All following figures in this section show drag compared to the reference drag, using the original geometry's reference as baseline for all CFD data, and the reference drag predicted by ESDU 81024 [1] for the output of the preliminary design code. The same set-up is used for all comparisons between CFD and ESDU-81024 predictions.

The spillage curve at Mach 0.5 shown in Figure 14 shows that the parametric geometry has consistently less drag than the original (about 1.3% of reference drag), and follows the latter at

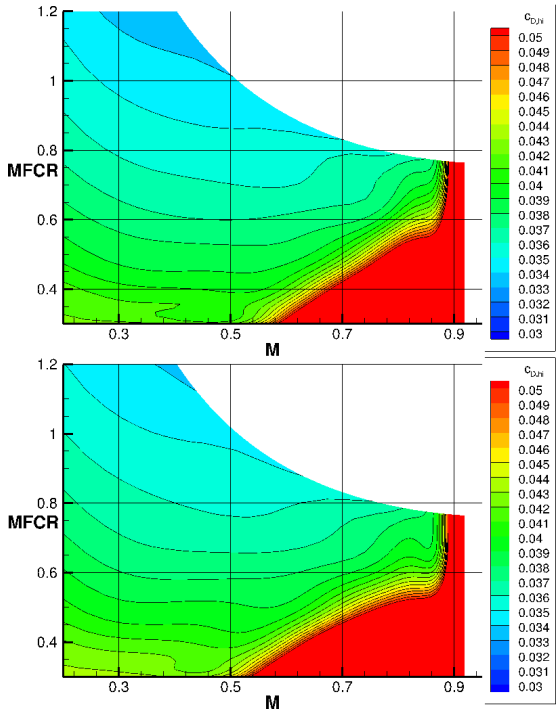

FIGURE 13: Drag maps of the reconstructed parametric (top) and the original (bottom) fan cowl geometry

almost constant offset. The ESDU-81024 prediction shows an increase in almost equal to the original fan cowl geometry, but also a very sharp increase in spillage drag at MFCR=0.55. This is related to the concept of "critical Mass-flow capture ratio" in the nacelle drag model used for the ESDU code [1], which assumes that at a certain MFCR the flow on the nacelle will separate and cause a large increase in drag. Large-scale separations were not observed in any of the CFD simulations presented here.

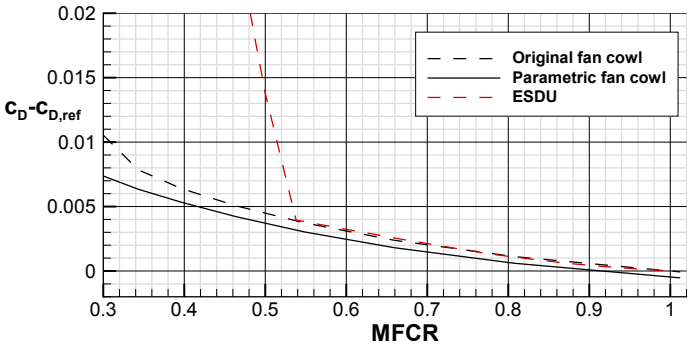

FIGURE 14: Comparison of spillage drag, at M=0.5 for the original and the reconstructed parametric shape, as well as predictions by the preliminary design code.

Figure 15 shows the drag rise curves at MFCR=0.75 and cruise Reynolds number. It can be seen that while the parametric geometry provides a slightly lower drag rise Mach number (by about 0.008), it has slightly lower drag below drag rise, by about 2%. The deviation of 0.008 in drag rise Mach number is the most significant difference between both fan cowls in terms of preliminary design, as it determines the maximum cruise Mach number at which a nacelle can be used. When using the parametric geometry and CFD process as a pure prediction tool, this deviation has relevance, although a preliminary design tool would be expected to be conservative. It should also be noted that the drag rise Mach number of the reconstructed design was achieved without any design work. The comparison of different initial forebody radii in previous sections has shown that a modest change to this variable alone may account for much of the observed difference. Regarding the lower-order model, the preliminary design code predicts drag rise at M=0.83, an error of 0.03. This can be attributed to the code's inability to regard other geometries than NACA1-forebodies at transonic Mach numbers, which limits the drag rise Mach numbers which can be achieved. The drag increase relative to reference drag predicted by the PD method is similar to that of the parametric nacelle.

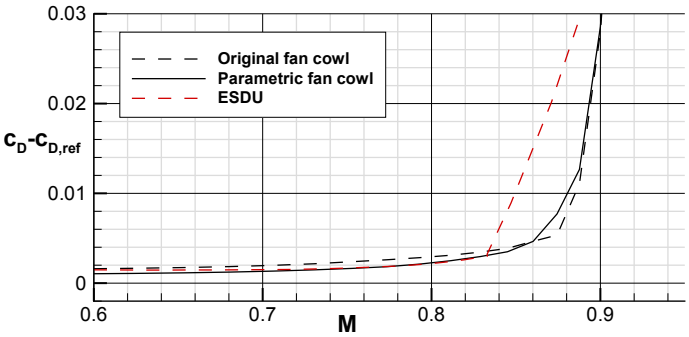

FIGURE 15: Comparison of drag rise curves for the original and the reconstructed parametric shape, at mid-cruise mass-flow capture ratio of 0.75, and prediction of the ESDU preliminary design method.

The spillage behaviour at transonic conditions is compared in Figure 16. The top graph shows curves at a constant Mach number of 0.82, below the drag rise predicted by the preliminary design code. The ESDU 81024 method predicts very little drag increase above MFCR=0.5, then but very strong increase at lower MFCR. In fact, the curve is almost equal to the one at M=0.5 in Figure 14. It can be seen that neither a sharp break in the spillage drag curve nor a similarity to the spillage curves at M=0.5 is reflected in the CFD results of either of the geometries. At M=0.85, the prediction of the preliminary design code cannot be usefully interpreted since the PD code assumes that the nacelle was already past wave drag rise. Between the two sets of CFD data, the parametric nacelle shows almost exactly the same drag as the original at MFCR=0.75 but has a slightly steeper drag increase. This results in a maximum deviation at around MFCR=0.55, of 4% at M=0.82 and 5% at M=0.85. At even lower MFCR, this drag difference reduces again, and both cases have equal drag at MFCR=0.4.

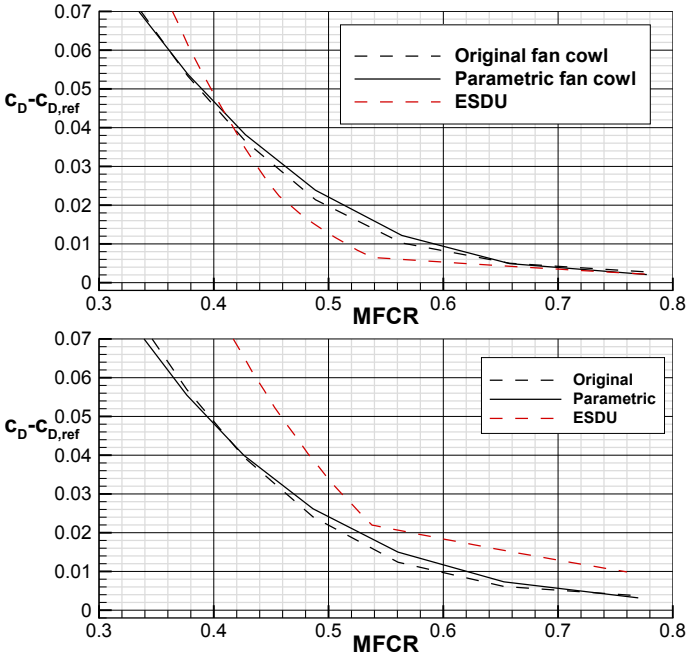

FIGURE 16: Comparison of spillage curves at M=0.82 (top) and M=0.85(bottom) for the original and the reconstructed parametric shape.

The observed differences in drag characteristic between the two fan cowl geometries are remarkably small. Overall drag rise Mach number and subsonic spillage are known to correlate reasonably well with the main dimensions of a fan cowl, such as thickness and length of the forebody. However, such correlations are hard to make for the specifics of drag increase at conditions when both wave drag and spillage are relevant, since the location of shocks depends on the specifics of curvature distribution. The parametric fan cowl is able to mimic the drag characteristics in far off-design conditions, only based on the main geometry measures shown in Table 1, and provides lower reference drag than the original design, without any design work.

The results show that it is possible to replicate the drag characteristics of a nacelle with good accuracy without any design work. This makes the parametric geometry not only a good concept for scenarios which require performance estimates based on a small number of input variables, but also as a starting point for

more detailed design, before moving on to full design optimisation with a larger number of design variables.

CONCLUSIONS

A parametric fan cowl shape was defined by 6 intuitive design variables as a tool to study preliminary design problems. It was complemented by a parametric intake geometry to allow CFD simulation of the flow over resulting nacelle geometries. The automated CFD process can simulate 224 operating conditions in less than 12 hours on a single compute node. This provides sufficient turnaround times for design space exploration.

The parametric geometry was shown to represent the aerodynamic properties of an existing nacelle design, based only on the 6 main geometry variables. It matches the properties of a through-flow nacelle (TFN) [18] with a maximum deviation of just 5%. At least for nacelles of similar proportions, the presented parametric shape can thus be regarded as representative of existing designs, both in terms of aerodynamic and geometric properties.

Predictions from the ESDU 81024 preliminary nacelle design code [1] in the transonic range are based on NACA1-type nacelles and show a much worse transonic performance, for all cases investigated. This underlines that the NACA1-type fan cowls are inadequate to represent modern-day transonic nacelles. Even at low Mach numbers, where the ESDU code uses a database which extends beyond the NACA1 forebody, the proposed parametric fan cowl shows lower spillage drag and no sharp drag increase from separation as predicted by the preliminary design code.

While these conclusions are subject to verification across a larger design space, the proposed parametric geometry and the associated CFD process appear to be suited as the basis for an improved preliminary design method, and as a tool for fast design space exploration.

The parametric CFD model links the main intuitive design variables of a nacelle to aerodynamic performance and changes in flow field topology and pressure distribution. This gives it some use beyond design space exploration, as a tool to study and understand nacelle aerodynamics in general. Given verification across a larger design space, the parametric shape may also be useful in cases where a placeholder geometry is needed to represent a realistic nacelle in a CFD simulation, without the time for an in-depth design.

ACKNOWLEDGEMENTS

This project was co-funded by Innovate UK.

REFERENCES

[1] ESDU, 1981. Drag of axisymmetric cowls at zero incidence for subsonic mach numbers. Tech. Rep. ESDU 81024, ESDU International, London, UK, November.

[2] E. L. Goldsmith, J. S., 1993. *Practical intake aerodynamic design*. Blackwell Scientific, Oxford.

[3] Kulfan, B. M., and Bussoletti, J. E., 2006. "Fundamental parametric geometry representations for aircraft component shapes". In 11th AIAA/ISSMO multidisciplinary analysis and optimization conference, Vol. 6948, sn.

[4] Ceze, M., Hayashi, M., and Volpe, E., 2009. "A study of the cst parameterization characteristics". In *27th AIAA Aplied Aerodynamics Conference*, no. AIAA 2009-3767. American Institute of Aeronautics and Astronautics, June.

[5] Sripawadkul, V., Padulo, M., and Guenov, M., 2010. "A comparison of airfoil shape parameterization techniques for early design optimization". In *13th AIAA/ISSMO Multidisciplinary Analysis Optimization Conference*, no. AIAA 2010-9050. American Institute of Aeronautics and Astronautics, Sept.

[6] Kulfan, B. M., 2008. "Universal parametric geometry representation method". *Journal of Aircraft,* ***45***(1), pp. 142–158.

[7] Hall, Z., Ahuja, V., Hartfield, R., Shelton, A., and Ahmed, A., 2009. "Optimization of a turbofan inlet duct using a genetic algorithm and cfd". In *27th AIAA Applied Aerodynamics Conference*, no. 2009-3775. AIAA, Jun.

[8] R. Christie, A. H., and MacManus, D., 2016. "An automated approach to nacelle parameterisation using intuitive class shape transformation curves". In ASME Turbo Expo, ASME. GT2016-57849.

[9] Langley, M., 1979. The design of axisymmetric cowls for podded nacelles for high by-pass ratio turbofan engines. Tech. Rep. Reports and memoranda No. 3846, Aircraft Research Association Ltd, Bedford.

[10] Zhu, F., and Qin, N., 2013. "Intuitive class/shape function parameterization for airfoils". *AIAA journal,* ***52***(1), pp. 17–25.

[11] ESDU, 1994. NACA 1-series geometry representation for computational fluid dynamics. Tech. Rep. ESDU-94013, ESDU, June.

[12] Fluent, A., 15. "Users guide, 2014".

[13] ANSYS, I. C. 15.0, users manual, ansys.

[14] Roache, P., 1998. *Verification and validation in computational science and engineering*. Hermosa publishers.

[15] Christie, R., Ramirez, S., and MacManus, D. G., 2014. "Aero-engine installation modelling and the impact on overall flight performance". In Advanced Aero Concepts, Design and Operations.

[16] MIDAP Study Group, 1979. Agardograph no. 237 guide to in-flight thrust measurement of turbojets and fan engines. Tech. Rep. AGARD-AG-237, AGARD.

[17] Langley, M., 1971. Measurements of external drag and surface pressure distributions on six cowls designed for high subsonic mach number. Tech. Rep. Model test note M.31/l, Parts l, 2 and 3, ARA.

[18] Vassberg, J. C., DeHaan, M. A., Rivers, S. M., and R. A. Wahls, R. A., 2008. "Development of a Common Research Model for Applied CFD Validation Studies". In 26th AIAA Applied Aerodynamics Conference, no. 6919, American Institute of Aeronautics and Astronautics, AIAA.

[19] AIAA, 2012. Common research model website. URL `http://commonresearchmodel.larc.nasa.gov`. Accessed: October 2015.

2016-09-20

Parametric geometry and CFD process for turbofan nacelles

Heidebrecht, Alexander

American Society of Mechanical Engineers